

J/ψ production at high transverse momenta in $p+p$
and Au+Au collisions at $\sqrt{s_{\text{NN}}} = 200$ GeV

The STAR Collaboration

L. Adamczyk¹, G. Agakishiev²¹, M. M. Aggarwal³⁴, Z. Ahammed⁵³,
A. V. Alakhverdyants²¹, I. Alekseev¹⁹, J. Alford²², C. D. Anson³¹,
D. Arkhipkin⁴, E. Aschenauer⁴, G. S. Averichev²¹, J. Balewski²⁶,
A. Banerjee⁵³, Z. Barnovska¹⁴, D. R. Beavis⁴, R. Bellwied⁴⁹,
M. J. Betancourt²⁶, R. R. Betts¹⁰, A. Bhasin²⁰, A. K. Bhati³⁴, H. Bichsel⁵⁵,
J. Bielcik¹³, J. Bielcikova¹⁴, L. C. Bland⁴, I. G. Bordyuzhin¹⁹,
W. Borowski⁴⁵, J. Bouchet²², A. V. Brandin²⁹, S. G. Brovko⁶, E. Bruna⁵⁷,
S. Bültmann³², I. Bunzarov²¹, T. P. Burton⁴, J. Butterworth⁴⁰, X. Z. Cai⁴⁴,
H. Caines⁵⁷, M. Calderón de la Barca Sánchez⁶, D. Cebra⁶, R. Cendejas⁷,
M. C. Cervantes⁴⁷, P. Chaloupka¹³, Z. Chang⁴⁷, S. Chattopadhyay⁵³,
H. F. Chen⁴², J. H. Chen⁴⁴, J. Y. Chen⁹, L. Chen⁹, J. Cheng⁵⁰,
M. Cherney¹², A. Chikanian⁵⁷, W. Christie⁴, P. Chung¹⁴, J. Chwastowski¹¹,
M. J. M. Codrington⁴⁷, R. Corliss²⁶, J. G. Cramer⁵⁵, H. J. Crawford⁵,
X. Cui⁴², S. Das¹⁶, A. Davila Leyva⁴⁸, L. C. De Silva⁴⁹, R. R. Debbé⁴,
T. G. Dedovich²¹, J. Deng⁴³, R. Derradi de Souza⁸, S. Dhamija¹⁸,
L. Didenko⁴, F. Ding⁶, A. Dion⁴, P. Djawotho⁴⁷, X. Dong²⁵,
J. L. Drachenberg⁴⁷, J. E. Draper⁶, C. M. Du²⁴, L. E. Dunkelberger⁷,
J. C. Dunlop⁴, L. G. Efimov²¹, M. Elnimr⁵⁶, J. Engelage⁵, G. Eppley⁴⁰,
L. Eun²⁵, O. Evdokimov¹⁰, R. Fatemi²³, S. Fazio⁴, J. Fedorisin²¹,
R. G. Fersch²³, P. Filip²¹, E. Finch⁵⁷, Y. Fisyak⁴, C. A. Gagliardi⁴⁷,
D. R. Gangadharan³¹, F. Geurts⁴⁰, A. Gibson⁵², S. Gliske²,
Y. N. Gorbunov¹², O. G. Grebenyuk²⁵, D. Grosnick⁵², S. Gupta²⁰,
W. Guryn⁴, B. Haag⁶, O. Hajkova¹³, A. Hamed⁴⁷, L.-X. Han⁴⁴,
J. W. Harris⁵⁷, J. P. Hays-Wehle²⁶, S. Heppelmann³⁵, A. Hirsch³⁷,
G. W. Hoffmann⁴⁸, D. J. Hofman¹⁰, S. Horvat⁵⁷, B. Huang⁴, H. Z. Huang⁷,
P. Huck⁹, T. J. Humanic³¹, L. Huo⁴⁷, G. Igo⁷, W. W. Jacobs¹⁸, C. Jena³⁰,
E. G. Judd⁵, S. Kabana⁴⁵, K. Kang⁵⁰, J. Kapitan¹⁴, K. Kauder¹⁰,
H. W. Ke⁹, D. Keane²², A. Kechechyan²¹, A. Kesich⁶, D. P. Kikola³⁷,
J. Kiryluk²⁵, I. Kisel²⁵, A. Kisiel⁵⁴, V. Kizka²¹, S. R. Klein²⁵,
D. D. Koetke⁵², T. Kollegger¹⁵, J. Konzer³⁷, I. Koralt³², L. Koroleva¹⁹,
W. Korsch²³, L. Kotchenda²⁹, P. Kravtsov²⁹, K. Krueger², I. Kulakov²⁵,
L. Kumar²², M. A. C. Lamont⁴, J. M. Landgraf⁴, S. LaPointe⁵⁶, J. Lauret⁴,

A. Lebedev⁴, R. Lednicky²¹, J. H. Lee⁴, W. Leight²⁶, M. J. LeVine⁴,
 C. Li⁴², L. Li⁴⁸, W. Li⁴⁴, X. Li³⁷, X. Li⁴⁶, Y. Li⁵⁰, Z. M. Li⁹, L. M. Lima⁴¹,
 M. A. Lisa³¹, F. Liu⁹, T. Ljubicic⁴, W. J. Llope⁴⁰, R. S. Longacre⁴, Y. Lu⁴²,
 X. Luo⁹, A. Luszczak¹¹, G. L. Ma⁴⁴, Y. G. Ma⁴⁴,
 D. M. M. D. Madagodagettige Don¹², D. P. Mahapatra¹⁶, R. Majka⁵⁷,
 O. I. Mall⁶, S. Margetis²², C. Markert⁴⁸, H. Masui²⁵, H. S. Matis²⁵,
 D. McDonald⁴⁰, T. S. McShane¹², S. Mioduszewski⁴⁷, M. K. Mitrovski⁴,
 Y. Mohammed⁴⁷, B. Mohanty³⁰, M. M. Mondal⁴⁷, B. Morozov¹⁹,
 M. G. Munhoz⁴¹, M. K. Mustafa³⁷, M. Naglis²⁵, B. K. Nandi¹⁷,
 Md. Nasim⁵³, T. K. Nayak⁵³, J. M. Nelson³, L. V. Nogach³⁶, J. Novak²⁸,
 G. Odyniec²⁵, A. Ogawa⁴, K. Oh³⁸, A. Ohlson⁵⁷, V. Okorokov²⁹,
 E. W. Oldag⁴⁸, R. A. N. Oliveira⁴¹, D. Olson²⁵, P. Ostrowski⁵⁴, M. Pachr¹³,
 B. S. Page¹⁸, S. K. Pal⁵³, Y. X. Pan⁷, Y. Pandit²², Y. Panebratsev²¹,
 T. Pawlak⁵⁴, B. Pawlik³³, H. Pei¹⁰, C. Perkins⁵, W. Peryt⁵⁴, P. Pile⁴,
 M. Planinic⁵⁸, J. Pluta⁵⁴, D. Plyku³², N. Poljak⁵⁸, J. Porter²⁵,
 A. M. Poskanzer²⁵, C. B. Powell²⁵, C. Pruneau⁵⁶, N. K. Pruthi³⁴,
 M. Przybycien¹, P. R. Pujahari¹⁷, J. Putschke⁵⁶, H. Qiu²⁵, R. Raniwala³⁹,
 S. Raniwala³⁹, R. L. Ray⁴⁸, R. Redwine²⁶, R. Reed⁶, C. K. Riley⁵⁷,
 H. G. Ritter²⁵, J. B. Roberts⁴⁰, O. V. Rogachevskiy²¹, J. L. Romero⁶,
 J. F. Ross¹², L. Ruan⁴, J. Rusnak¹⁴, N. R. Sahoo⁵³, P. K. Sahu¹⁶,
 I. Sakrejda²⁵, S. Salur²⁵, A. Sandacz⁵⁴, J. Sandweiss⁵⁷, E. Sangaline⁶,
 A. Sarkar¹⁷, J. Schambach⁴⁸, R. P. Scharenberg³⁷, A. M. Schmah²⁵,
 B. Schmidke⁴, N. Schmitz²⁷, T. R. Schuster¹⁵, J. Seele²⁶, J. Seger¹²,
 P. Seyboth²⁷, N. Shah⁷, E. Shahaliev²¹, M. Shao⁴², B. Sharma³⁴,
 M. Sharma⁵⁶, S. S. Shi⁹, Q. Y. Shou⁴⁴, E. P. Sichtermann²⁵,
 R. N. Singaraju⁵³, M. J. Skoby¹⁸, D. Smirnov⁴, N. Smirnov⁵⁷, D. Solanki³⁹,
 P. Sorensen⁴, U. G. deSouza⁴¹, H. M. Spinka², B. Srivastava³⁷,
 T. D. S. Stanislaus⁵², S. G. Steadman²⁶, J. R. Stevens¹⁸, R. Stock¹⁵,
 M. Strikhanov²⁹, B. Stringfellow³⁷, A. A. P. Suaide⁴¹, M. C. Suarez¹⁰,
 M. Sumbera¹⁴, X. M. Sun²⁵, Y. Sun⁴², Z. Sun²⁴, B. Surrow⁴⁶,
 D. N. Svirida¹⁹, T. J. M. Symons²⁵, A. Szanto de Toledo⁴¹, J. Takahashi⁸,
 A. H. Tang⁴, Z. Tang⁴², L. H. Tarini⁵⁶, T. Tarnowsky²⁸, D. Thein⁴⁸,
 J. H. Thomas²⁵, J. Tian⁴⁴, A. R. Timmins⁴⁹, D. Tlusty¹⁴, M. Tokarev²¹,
 S. Trentalange⁷, R. E. Tribble⁴⁷, P. Tribedy⁵³, B. A. Trzeciak⁵⁴,
 O. D. Tsai⁷, J. Turnau³³, T. Ullrich⁴, D. G. Underwood², G. Van Buren⁴,
 G. van Nieuwenhuizen²⁶, J. A. Vanfossen, Jr.²², R. Varma¹⁷,
 G. M. S. Vasconcelos⁸, F. Videbæk⁴, Y. P. Vijoyi⁵³, S. Vokal²¹,
 S. A. Voloshin⁵⁶, A. Vossen¹⁸, M. Wada⁴⁸, F. Wang³⁷, G. Wang⁷, H. Wang⁴,

J. S. Wang²⁴, Q. Wang³⁷, X. L. Wang⁴², Y. Wang⁵⁰, G. Webb²³,
 J. C. Webb⁴, G. D. Westfall²⁸, C. Whitten Jr.⁷, H. Wieman²⁵,
 S. W. Wissink¹⁸, R. Witt⁵¹, W. Witzke²³, Y. F. Wu⁹, Z. Xiao⁵⁰, W. Xie³⁷,
 K. Xin⁴⁰, H. Xu²⁴, N. Xu²⁵, Q. H. Xu⁴³, W. Xu⁷, Y. Xu⁴², Z. Xu⁴, L. Xue⁴⁴,
 Y. Yang²⁴, Y. Yang⁹, P. Yepes⁴⁰, Y. Yi³⁷, K. Yip⁴, I-K. Yoo³⁸,
 M. Zawisza⁵⁴, H. Zbroszczyk⁵⁴, J. B. Zhang⁹, S. Zhang⁴⁴, X. P. Zhang⁵⁰,
 Y. Zhang⁴², Z. P. Zhang⁴², F. Zhao⁷, J. Zhao⁴⁴, C. Zhong⁴⁴, X. Zhu⁵⁰,
 Y. H. Zhu⁴⁴, Y. Zoukarneeva²¹, M. Zyzak²⁵

¹*AGH University of Science and Technology, Cracow, Poland*

²*Argonne National Laboratory, Argonne, Illinois 60439, USA*

³*University of Birmingham, Birmingham, United Kingdom*

⁴*Brookhaven National Laboratory, Upton, New York 11973, USA*

⁵*University of California, Berkeley, California 94720, USA*

⁶*University of California, Davis, California 95616, USA*

⁷*University of California, Los Angeles, California 90095, USA*

⁸*Universidade Estadual de Campinas, Sao Paulo, Brazil*

⁹*Central China Normal University (HZNU), Wuhan 430079, China*

¹⁰*University of Illinois at Chicago, Chicago, Illinois 60607, USA*

¹¹*Cracow University of Technology, Cracow, Poland*

¹²*Creighton University, Omaha, Nebraska 68178, USA*

¹³*Czech Technical University in Prague, FNSPE, Prague, 115 19, Czech Republic*

¹⁴*Nuclear Physics Institute AS CR, 250 68 Řež/Prague, Czech Republic*

¹⁵*University of Frankfurt, Frankfurt, Germany*

¹⁶*Institute of Physics, Bhubaneswar 751005, India*

¹⁷*Indian Institute of Technology, Mumbai, India*

¹⁸*Indiana University, Bloomington, Indiana 47408, USA*

¹⁹*Alikhanov Institute for Theoretical and Experimental Physics, Moscow, Russia*

²⁰*University of Jammu, Jammu 180001, India*

²¹*Joint Institute for Nuclear Research, Dubna, 141 980, Russia*

²²*Kent State University, Kent, Ohio 44242, USA*

²³*University of Kentucky, Lexington, Kentucky, 40506-0055, USA*

²⁴*Institute of Modern Physics, Lanzhou, China*

- ²⁵Lawrence Berkeley National Laboratory, Berkeley, California 94720, USA
- ²⁶Massachusetts Institute of Technology, Cambridge, MA 02139-4307, USA
- ²⁷Max-Planck-Institut für Physik, Munich, Germany
- ²⁸Michigan State University, East Lansing, Michigan 48824, USA
- ²⁹Moscow Engineering Physics Institute, Moscow Russia
- ³⁰National Institute of Science and Education and Research, Bhubaneswar 751005, India
- ³¹Ohio State University, Columbus, Ohio 43210, USA
- ³²Old Dominion University, Norfolk, VA, 23529, USA
- ³³Institute of Nuclear Physics PAN, Cracow, Poland
- ³⁴Panjab University, Chandigarh 160014, India
- ³⁵Pennsylvania State University, University Park, Pennsylvania 16802, USA
- ³⁶Institute of High Energy Physics, Protvino, Russia
- ³⁷Purdue University, West Lafayette, Indiana 47907, USA
- ³⁸Pusan National University, Pusan, Republic of Korea
- ³⁹University of Rajasthan, Jaipur 302004, India
- ⁴⁰Rice University, Houston, Texas 77251, USA
- ⁴¹Universidade de Sao Paulo, Sao Paulo, Brazil
- ⁴²University of Science & Technology of China, Hefei 230026, China
- ⁴³Shandong University, Jinan, Shandong 250100, China
- ⁴⁴Shanghai Institute of Applied Physics, Shanghai 201800, China
- ⁴⁵SUBATECH, Nantes, France
- ⁴⁶Temple University, Philadelphia, Pennsylvania, 19122
- ⁴⁷Texas A&M University, College Station, Texas 77843, USA
- ⁴⁸University of Texas, Austin, Texas 78712, USA
- ⁴⁹University of Houston, Houston, TX, 77204, USA
- ⁵⁰Tsinghua University, Beijing 100084, China
- ⁵¹United States Naval Academy, Annapolis, MD 21402, USA
- ⁵²Valparaiso University, Valparaiso, Indiana 46383, USA
- ⁵³Variable Energy Cyclotron Centre, Kolkata 700064, India
- ⁵⁴Warsaw University of Technology, Warsaw, Poland

⁵⁵ *University of Washington, Seattle, Washington 98195, USA*

⁵⁶ *Wayne State University, Detroit, Michigan 48201, USA*

⁵⁷ *Yale University, New Haven, Connecticut 06520, USA*

⁵⁸ *University of Zagreb, Zagreb, HR-10002, Croatia*

Abstract

We report J/ψ spectra for transverse momenta $p_T > 5$ GeV/ c at mid-rapidity in $p+p$ and Au+Au collisions at $\sqrt{s_{NN}} = 200$ GeV. The inclusive J/ψ spectrum and the extracted B -hadron feed-down are compared to models incorporating different production mechanisms. We observe significant suppression of the J/ψ yields for $p_T > 5$ GeV/ c in 0-30% central Au+Au collisions relative to the $p+p$ yield scaled by the number of binary nucleon-nucleon collisions in Au+Au collisions. In 30-60% mid-central collisions, no such suppression is observed. The level of suppression is consistently less than that of high- p_T π^\pm and low- p_T J/ψ at RHIC and high- p_T J/ψ at the LHC.

Keywords: J/ψ suppression, color-screening, quarkonium, heavy-ion collisions, STAR

1. Introduction

Ultrarelativistic heavy-ion collisions provide a unique environment to study strongly interacting matter at high temperature and energy density where a transition from the hadronic phase of matter to a new partonic phase, the Quark-Gluon Plasma (QGP), takes place. Measurements of the in-medium dissociation probability of the different quarkonium states are expected to provide an estimate of the initial temperature of the system [1, 2, 3]. The J/ψ is the lightest and most abundantly produced quarkonium state accessible in experiment. However, significant decay contributions ($\approx 40\%$ [2]) from excited $c\bar{c}$ states, such as the χ_c and $\psi(2S)$, and from B mesons could complicate the suppression picture suggested by dissociation models [4]. In addition, other contributions absent in $p+p$ collisions are likely to have a significant impact on the observed J/ψ yields in relativistic heavy-ion collisions

at CERN-SPS [5], BNL-RHIC [6] and CERN-LHC [7, 8, 9]. These contributions include cold nuclear matter (CNM) effects such as initial state parton scattering, nuclear shadowing and nuclear absorption, the combined contribution of finite J/ψ formation time and the finite space-time extent of the hot and dense volume where the dissociation can occur, and recombination of unassociated c and \bar{c} in the medium [10]. Some of these processes are expected to decrease with increasing J/ψ p_T [11, 12]. It is therefore anticipated that J/ψ measurements at high- p_T provide an important tool to decouple some of the mechanisms mentioned above and provide a cleaner way to extract the contribution from color-screening effects [11, 12, 13, 14]. Our previous J/ψ measurements are consistent with no suppression for $p_T > 5$ GeV/ c in Cu+Cu collisions at $\sqrt{s_{NN}} = 200$ GeV, to within the limited precision of the data [15]. The small system size created in Cu+Cu collisions may result in high- p_T J/ψ formation outside the medium. Precise measurements in Au+Au collisions are thus crucial for a systematic study of J/ψ production in the hot and dense medium.

The interpretation of medium-induced J/ψ modification requires a good understanding of its production mechanisms in $p+p$ collisions, which include direct production via gluon fusion, parton fragmentation, and feed-down from higher charmonium states and B -hadron decays [4]. The initial hard interactions required to create the charm quark pairs can be well calculated in perturbative QCD (pQCD). However, the subsequent soft processes required to form the J/ψ hadron and the J/ψ formation time are theoretically not well understood [4]. No model at present fully explains the J/ψ observations in elementary collisions [4]. The J/ψ spectrum in the intermediate and high- p_T range, together with the angular correlations of a high- p_T J/ψ and associated charged hadrons, may provide additional insights in the underlying production mechanisms.

In this letter, we report a measurement of J/ψ production for $2 < p_T < 14$ GeV/ c in $p+p$ and Au+Au collisions at $\sqrt{s_{NN}} = 200$ GeV with the STAR detector [16]. The J/ψ p_T spectra at mid-rapidity ($|y| < 1$) in $p+p$ and Au+Au collisions are presented. The nuclear modification factor, R_{AA} – the ratio of the yield in Au+Au to that in $p+p$ collisions scaled by the number of underlying binary nucleon-nucleon collisions (N_{bin} – is calculated and compared to theoretical calculations.

2. Data analysis

The Au+Au data used for this analysis were recorded in 2010, and the $p+p$ data in 2009. The minimum bias (MB) trigger was defined to be a coincidence of the two Vertex Position Detectors [17]. Online trigger conditions that utilized a MB trigger condition and two thresholds for the energy deposited in any single Barrel Electromagnetic Calorimeter (BEMC) [18] tower, with a size of $\Delta\eta \times \Delta\phi = 0.05 \times 0.05$, were used to maximize the sampled luminosity. To increase the trigger efficiency, the $p+p$ data with high BEMC threshold were recorded without a MB requirement. The $p+p$ data with low BEMC threshold were pre-scaled to keep the data rate manageable. The integrated luminosities of the data samples used for this analysis are 23.1 pb^{-1} and 1.8 pb^{-1} with a transverse energy threshold of $E_T > 6.0$ and 2.6 GeV , respectively, in $p+p$ collisions and 1.4 nb^{-1} with $E_T > 4.3 \text{ GeV}$ in Au+Au collisions. In the Au+Au data, the collision centrality is determined by the distribution of charged-particle multiplicity within the pseudorapidity range $|\eta| < 0.5$ [19].

In this analysis, $J/\psi \rightarrow e^+e^-$ decays were reconstructed using the STAR Time Projection Chamber (TPC) [21] and the BEMC [18] with full azimuthal coverage over the pseudorapidity range $|\eta| < 1$ [15, 22]. Electron identification (eID) for the BEMC triggered tracks was achieved by measuring the ionization energy loss (dE/dx) and track momentum from the TPC, as well as the energy deposition in the BEMC. In addition, the shower profile in the barrel shower maximum detector [18] was used in Au+Au collisions to further suppress hadron contamination. At moderate p_T ($1 \lesssim p_T \lesssim 3 \text{ GeV}/c$), TPC dE/dx provides eID with reasonable efficiency and purity. At low p_T ($0.2 < p_T \lesssim 3 \text{ GeV}/c$), the eID significantly benefits from a recently installed large area time-of-flight (TOF) detector covering $|\eta| < 0.9$ [23, 24]. The complete TOF detector was available for the 2010 Au+Au run, whereas 72% was available for the $p+p$ data collected in 2009.

The J/ψ signal was extracted by subtracting from the unlike-sign ee invariant mass spectrum the random combinatorial background that was reproduced by the like-sign spectrum in $p+p$ collisions and unlike-sign spectrum from mixed-events in Au+Au collisions [25]. Figure 1 shows the invariant mass distribution before and after the combinatorial background subtraction in $p+p$ and Au+Au collisions at $\sqrt{s_{\text{NN}}} = 200 \text{ GeV}$. The J/ψ raw yields were obtained from a mass window of $2.7 < M_{inv}^{ee} < 3.3 - 3.4 \text{ GeV}/c^2$ in $p+p$ collisions depending on the J/ψ p_T , and $2.9 < M_{inv}^{ee} < 3.2 \text{ GeV}/c^2$ in Au+Au

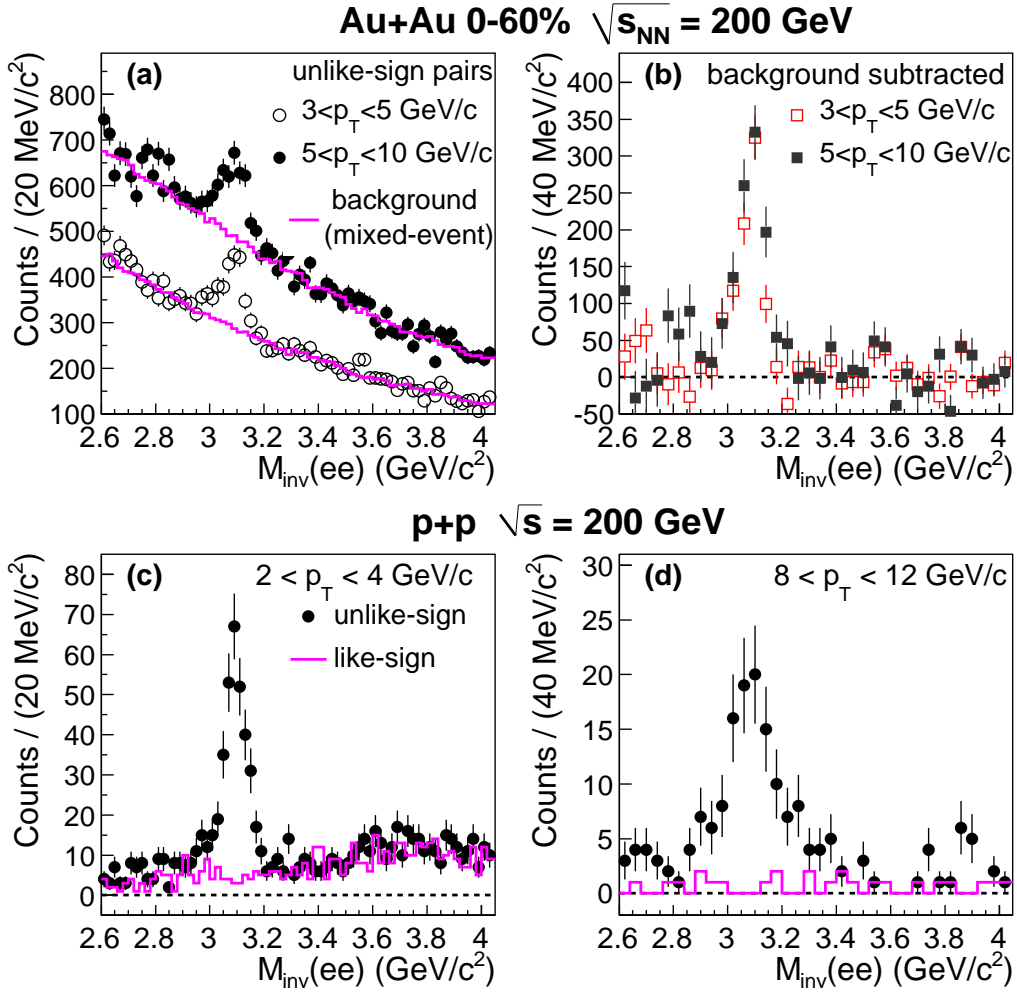


Figure 1: (Color online.) (a) The unlike-sign e^+e^- invariant mass distribution from same-event pairs (filled circles) and mixed-event pairs (solid curve) in Au+Au collisions at $\sqrt{s_{NN}} = 200$ GeV. (b) The background subtracted e^+e^- invariant mass distribution in Au+Au collisions at $\sqrt{s_{NN}} = 200$ GeV. (c, d) The unlike-sign (filled circles) and like-sign (solid curve) ee invariant mass distribution from same-event pairs in $p+p$ collisions at $\sqrt{s} = 200$ GeV. For both systems the data are shown for two intervals in J/ψ p_T .

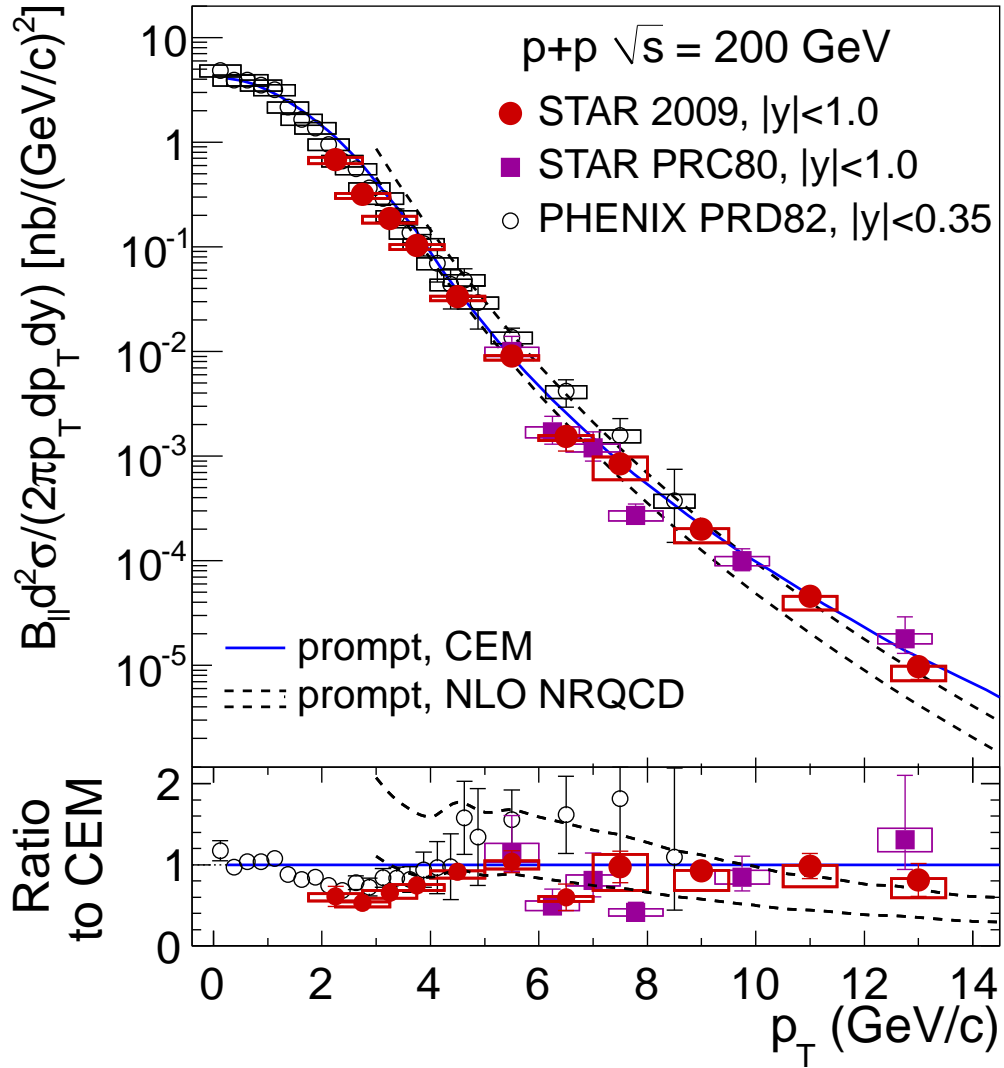


Figure 2: (Color online.) The invariant J/ψ cross section versus p_T in $p+p$ collisions at $\sqrt{s} = 200$ GeV. The vertical bars and boxes depict the statistical and systematic uncertainties, respectively. Also shown are results published by STAR [15] and PHENIX [20]. The curves show theoretical calculations described in the text.

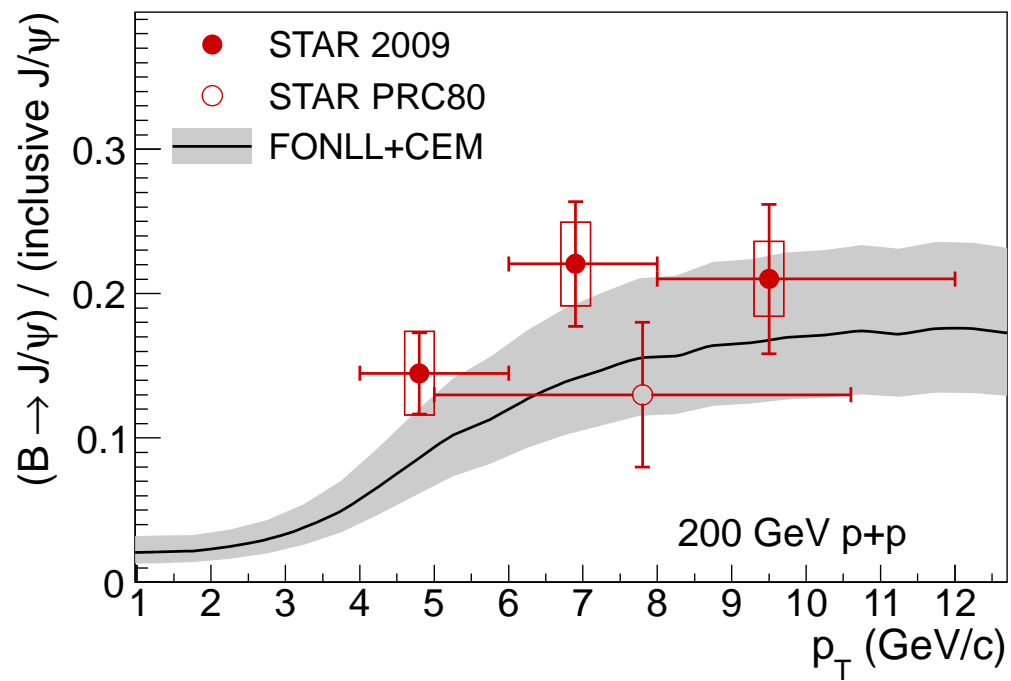


Figure 3: (Color online.) The fraction of $B \rightarrow J/\psi$ over the inclusive J/ψ yield in $p+p$ collisions. The FONLL+CEM model calculation is also shown.

Table 1: Summary of assigned systematic uncertainties of J/ψ spectra in $p+p$ and Au+Au collisions, and $J/\psi R_{AA}$ in Au+Au collisions.

Description	$p+p$	Au+Au	R_{AA}
Kinematic and eID cuts	1-16%	3-28%	3-28%
Efficiency	7.5%	7.5%	-
Yield extraction	8-26%	2%	4%
Normalization	8.1%	-	8.6-23.4%

collisions. The yields were corrected for $\approx 10\%$ radiation losses that cause some of the decay daughters to be reconstructed with M_{inv}^{ee} outside the above mass ranges. The total J/ψ yield was ≈ 1100 ($p_T > 2$ GeV/ c) in $p+p$ collisions. It was ≈ 1000 , 600 and 300 ($p_T > 3$ GeV/ c) in 0-20%, 20-40% and 40-60% Au+Au collisions, respectively. The signal to background ratio (S/B) was ≈ 4 in $p+p$ collisions and $\approx 1/7$ (1/2) in 0-20% (40-60%) Au+Au collisions. In the J/ψ -hadron correlation analysis, different invariant mass and particle identification cuts were selected to provide a better S/B ratio. About 400 J/ψ with $p_T > 4$ GeV/ c and $3.0 < M_{inv}^{ee} < 3.2$ GeV/ c^2 were observed with a S/B ratio of 22/1 in $p+p$ collisions.

Acceptance and efficiency corrections were studied using Monte Carlo (MC) GEANT simulations [19]. The systematic uncertainty on this procedure is estimated by varying kinematic and eID cuts in both data analysis and MC simulations. It is uncorrelated with p_T and collisions systems. An additional systematic uncertainty of 7.5%, obtained from two complementary simulation methods, was assigned for the p_T spectra in $p+p$ and Au+Au collisions. This contribution cancels in the uncertainty on R_{AA} . We have also varied the invariant mass window for signal counting to evaluate the systematic uncertainty on the yield extraction procedure, including the contributions from radiation losses and correlated background. This contribution is larger in $p+p$ than in Au+Au collisions due to the wider mass window used in $p+p$ collisions. Since it is correlated in $p+p$ and Au+Au collisions, this systematic uncertainty on R_{AA} is estimated by varying the mass window in the same way in $p+p$ and Au+Au collisions. The normalization uncertainty for the cross section in $p+p$ collisions is 8.1% [26]. The normalization uncertainty for R_{AA} has also a contribution from the uncertainty on the calculation of N_{bin} . The combined uncertainty varies from 8.6% in 0-10% central Au+Au collisions to 23.4% in 40-60% central Au+Au collisions. The systematic uncertainties are summarized in Tab. 1.

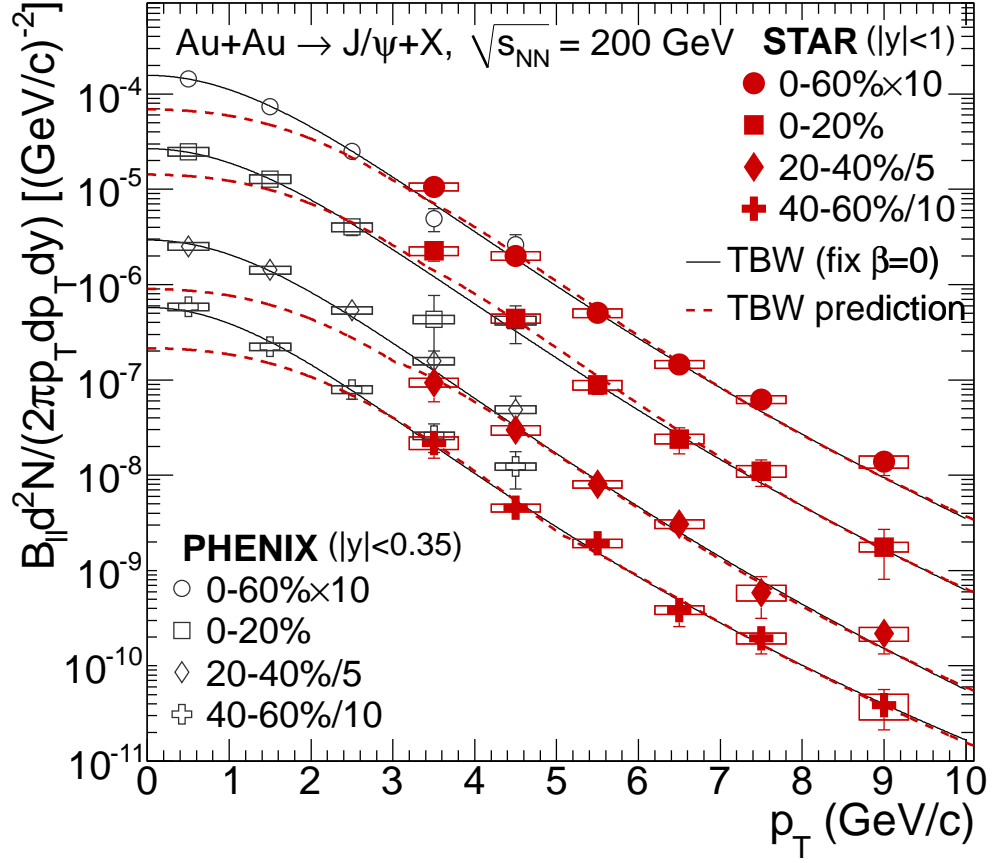


Figure 4: (Color online) J/ψ p_T distributions in Au+Au collisions with different centralities at $\sqrt{s_{NN}} = 200$ GeV. For clarity, the data and curves have been scaled as indicated in the legends. The PHENIX results are reported in [6]. The curves are model fits described in the text.

3. Results and discussion

Figure 2 shows the J/ψ invariant cross-section times the branching ratio (B_U) [27] at mid-rapidity ($|y| < 1$) as a function of p_T for $p+p$ collisions at $\sqrt{s} = 200$ GeV. The new results are consistent with those previously published by STAR [15] and PHENIX [20]. The dashed curves depict the uncertainty band of next-to-leading order (NLO) theoretical Non-Relativistic QCD (NRQCD) calculations from color-octet (CO) and color-singlet (CS) transitions [28] for prompt J/ψ production in $p+p$ collisions. The CS+CO calculations match the p_T spectra for $p_T > 4$ GeV/ c to within the uncertainties. The solid curve shows the calculation from the color evaporation model (CEM) for prompt J/ψ [29]. It describes the p_T spectra reasonably well at low and high p_T , but overpredicts the data by a factor of 2 at p_T around 3 GeV/ c . The bottom panel shows the ratios of the data and NRQCD calculations to the CEM calculation. Not shown in this figure is the model based on NNLO* CS [30], which predicts a too steep p_T dependence, as discussed in [15].

The relative contribution of B -hadron feed-down to the inclusive J/ψ yield was obtained by fitting the azimuthal angular correlation between high- p_T J/ψ and charged hadrons with simulated correlation functions for prompt J/ψ and J/ψ from B -hadron feed-down from PYTHIA [31, 32]. Details of this procedure are described in [15, 22]. The separation of the correlation functions for the two above contribution sources increases as a function of p_T . We note that this method is data-driven, although it relies also on the validity of PYTHIA's modeling of the near-side associated hadron distributions. The B -hadron feed-down contribution is found to be within 10-25% in the range $4 < p_T < 12$ GeV/ c as shown in Fig. 3. Within errors our data are consistent with the Fixed Order plus Next-to-Leading Logarithms (FONLL) plus CEM prediction [33, 34] indicated by the curve and uncertainty band. More precise measurements using displaced vertex techniques [35] similar to those employed by CDF in $p + \bar{p}$ collisions at $\sqrt{s} = 1.96$ TeV and by ATLAS and CMS in $p+p$ collisions at $\sqrt{s} = 7$ TeV [36, 37, 38] are needed to quantify the anticipated energy dependence [33, 34].

The measured J/ψ p_T spectra in Au+Au collisions for different centralities are shown in Fig. 4. The shape of the J/ψ p_T -distribution depends not only on the production mechanism but in heavy ion collisions also on the level of charm quark thermalization. J/ψ produced from direct pQCD processes have no initial collective motion and may acquire radial flow through interaction with the hot and dense medium. J/ψ produced from charm

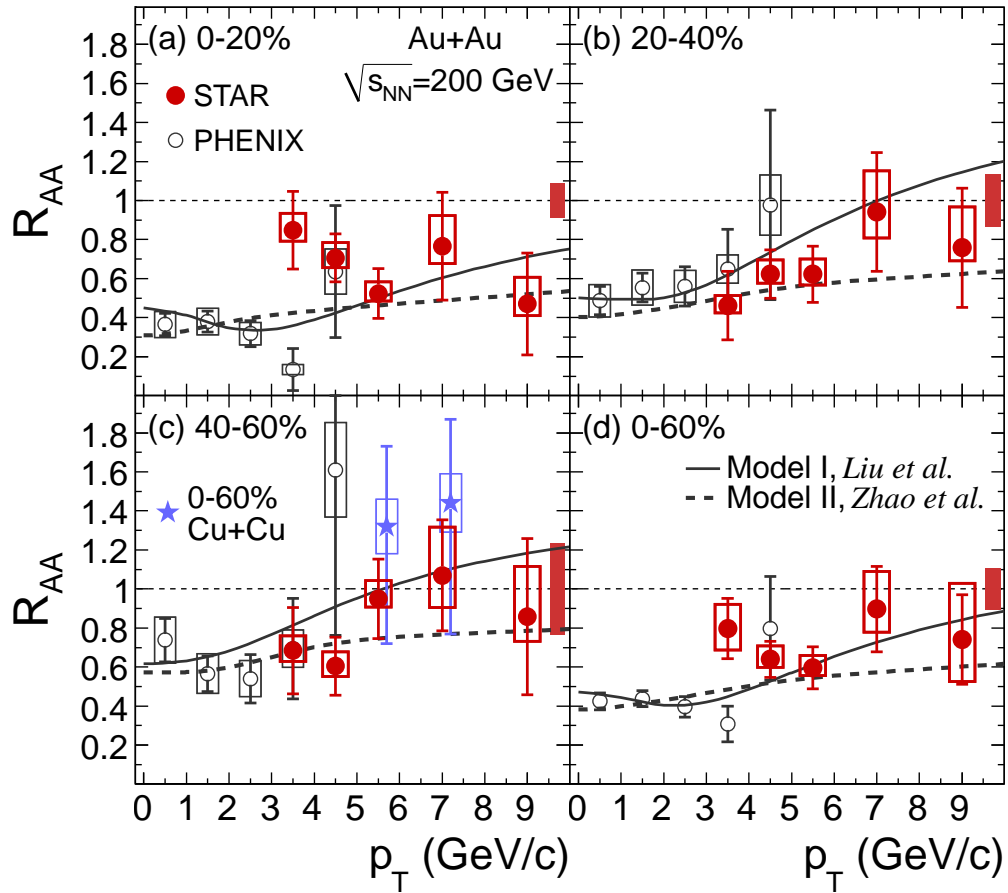


Figure 5: (Color online.) J/ψ R_{AA} versus p_T for several centrality bins for Au+Au collisions at $\sqrt{s_{NN}} = 200$ GeV. The statistical (systematic) uncertainties are shown with vertical bars (open boxes). The filled boxes about unity on the right show the size of the normalization uncertainty. PHENIX low- p_T J/ψ results [6] and STAR high- p_T results in Cu+Cu collisions [15] are shown for comparison. The curves are from the predictions by Model I (Liu et al.) [11] and Model II (Zhao et al.) [12].

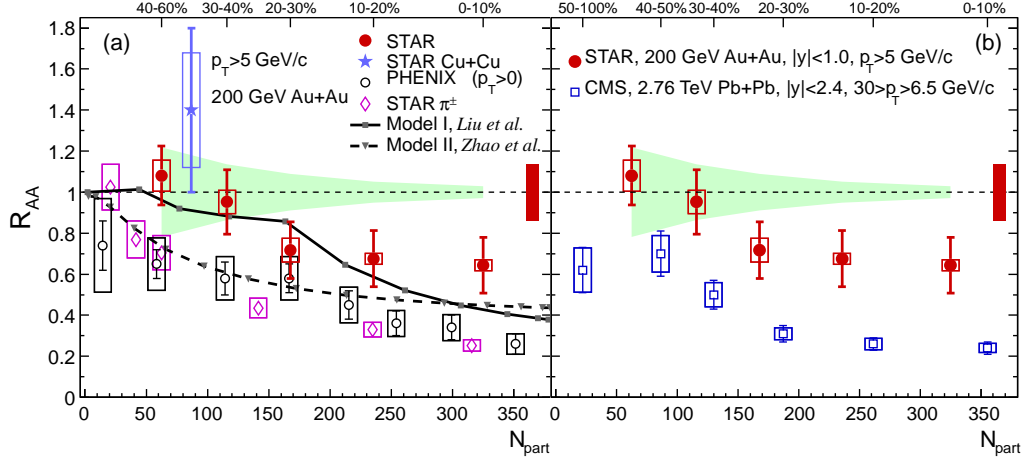


Figure 6: (Color online) R_{AA} versus N_{part} for high- p_T J/ψ in comparison with a) low- p_T J/ψ data from PHENIX [6], and high- p_T π^\pm from STAR [41, 42], and b) high- p_T J/ψ from CMS [8]. The statistical (systematic) uncertainties are shown in vertical bars (boxes). The shaded green band about unity shows the systematic uncertainties from N_{bin} and the box about unity on the right shows the R_{AA} normalization uncertainty from the statistical and global systematic uncertainties of the $p+p$ reference data. The percentage in the top horizontal axis of (a) and (b) refer to the collision centrality for high- p_T J/ψ data at the RHIC and LHC, respectively.

quark recombination should inherit the flow of charm quarks and exhibit an enhancement of yield at low p_T . Thus the study of J/ψ p_T spectra with a thermal model may provide insight in its production mechanism and thermalization. The solid curves depict fits based on the Tsallis statistics Blast-wave (TBW) model to the combined STAR and PHENIX data with the radial flow velocity β fixed to zero [39]. The fits reproduce the data reasonably well. Under the assumption that the J/ψ flows like light hadrons [39, 40], the TBW calculations shown as dashed curves underpredict the yields at low p_T . This could be due to a small (or zero) radial flow or a significant contribution from charm quark recombination that would enhance the yield at low p_T , or both.

Figure 5 shows the J/ψ R_{AA} versus p_T for different centrality bins. The STAR Cu+Cu J/ψ results [15] are also shown. For $p_T > 5$ GeV/c, J/ψ R_{AA} in the 40-60% centrality bin is consistent with unity and with our previous measurement in Cu+Cu collisions with a similar average number of participants (N_{part}). The curves show two theoretical calculations [11, 12] describing the

data reasonably well. These calculations include contributions from prompt production and statistical charm quark regeneration. The suppression of the prompt J/ψ component in the model calculations is mainly due to the color-screening effect. The model from Zhao et al. (Model II) [12] also includes the J/ψ formation-time effect and the B -hadron feed-down contribution.

For $p_T > 5$ GeV/ c , J/ψ production follows the scaling of the cross section at mid-rapidity, $\frac{d^2\sigma}{2\pi p_T dp_T dy} = g(x_T)/(\sqrt{s})^n$, where $x_T = 2p_T/\sqrt{s}$ and $g(x_T)$ is a universal function of x_T [43, 44, 45, 46] observed for a wide range of collision energies and confirmed by STAR data on $p+p$ collisions at $\sqrt{s} = 200$ GeV [15]. It has been argued that the breaking of x_T scaling at low p_T ($p_T \approx 2$ GeV/ c) for hadrons (pions and protons) [15, 44, 45, 46] indicates a possible transition from soft to hard processes and thus defines the range where pQCD is applicable. Similarly, the observed x_T scaling behavior of the J/ψ suggests a transition from soft to hard process at around $p_T \approx 5$ GeV/ c . In the high p_T region, the CNM and $c\bar{c}$ recombination effects are expected to be negligible in heavy-ion collisions [11, 12]. By consequence, J/ψ suppression in this p_T region should provide a cleaner probe of the hot medium suppression effects. Furthermore, a color-screening model based on AdS/CFT predicts that the dissociation temperature of direct J/ψ in QGP decreases to $1.5 T_c$, which is believed to be reached in RHIC collisions, at $p_T > 5$ GeV/ c [13].

We present high- p_T ($p_T > 5$ GeV/ c) R_{AA} as a function of N_{part} in Fig. 6. No significant suppression of high- p_T J/ψ production is observed in mid-central to peripheral collisions (30-60%, $N_{part} \lesssim 140$). However, in central collisions (0-30%, $N_{part} \gtrsim 140$), high- p_T J/ψ are significantly suppressed. The R_{AA} of low- p_T ($0 < p_T < 5$ GeV/ c) J/ψ measured by PHENIX [6] and high- p_T ($p_T > 5$ GeV/ c) charged pions measured by STAR [41, 42] are shown in Fig. 6(a) for comparison. The high- p_T J/ψ R_{AA} is systematically higher. Note, that the B -hadron feed-down contribution is not subtracted and that part of the suppression could for instance reflect b -quark energy loss. Based on our measurement, R_{AA} for prompt J/ψ with $p_T > 5$ GeV/ c in the most central collisions will be 0.80 ± 0.17 if B -hadron $R_{AA} = 0$ and 0.55 ± 0.17 if B -hadron $R_{AA} = 1$. The predictions of high- p_T J/ψ R_{AA} from Model I (Liu et al.) [47] and Model II (Zhao et al.) [12] are shown as solid and dashed curves, respectively. Model I describes our data reasonably well. Model II underpredicts J/ψ R_{AA} (p -value=0.0018 with all of the uncertainties taken into account). Fig. 6(b) shows the comparison of high- p_T J/ψ R_{AA} versus

N_{part} from STAR at RHIC and CMS at the LHC [8]. The STAR results are higher for all centralities.

The high- p_T J/ψ R_{AA} versus centrality is different from that of high- p_T pions. This is expected from differences in their production. Dissociation is considered to be the dominant mechanism that determines the R_{AA} in the case of J/ψ production, and induced gluon radiation in the case of pion production. For $p_T > 5$ GeV/ c , the recombination and initial parton scattering effects are expected to be negligible [11, 12]. The observed J/ψ R_{AA} dependence on system size in this p_T range might be due to the interplay of formation time, color screening and parton distribution functions in heavy nuclei [10]. The model calculations of [12] include formation time effects and CNM effects, and predict that J/ψ R_{AA} is close to unity for $p_T > 5$ GeV/ c . Therefore significant suppression observed in central 0-30% Au+Au collisions points to the color screening features. Empirically, the J/ψ is the only measured hadron that exhibits significant suppression in R_{AA} and has neither observable elliptic flow [48] nor model-extracted radial flow [39] at RHIC. The strong suppression of J/ψ at high p_T and the sequential Υ suppression observed at LHC by the CMS Collaboration [8, 49, 50] are consistent with this interpretation. Comparison of low- p_T J/ψ yields at RHIC and LHC [51] and study of the J/ψ azimuthal anisotropy [48, 52] could quantitatively further constrain the model interpretation.

4. Summary

This letter reports measurements of J/ψ production in $\sqrt{s_{NN}} = 200$ GeV $p+p$ and Au+Au collisions for $p_T > 2-3$ GeV/ c at RHIC. The p_T spectrum in $p+p$ collisions is compared to various theoretical calculations. Currently, only the CEM model and NLO CS+CO calculation describe our data. Based on the measurement of azimuthal correlations between high- p_T J/ψ and charged hadrons we estimate the fraction of J/ψ from B -hadron decay to be 10-25% in the p_T range of 4-12 GeV/ c in $p+p$ collisions. We report the first measurement of high- p_T J/ψ suppression in Au+Au collisions at RHIC. The nuclear modification factor R_{AA} in Au+Au increases from low to high p_T . For $p_T > 5$ GeV/ c , J/ψ R_{AA} is consistent with no suppression from mid-central to peripheral collisions (30-60% centrality), and significantly smaller than unity in the most central Au+Au collisions. The results on R_{AA} versus p_T and N_{part} provide new insight in the study of color screening features for charmonium.

Acknowledgments

We thank the RHIC Operations Group and RCF at BNL, the NERSC Center at LBNL and the Open Science Grid consortium for providing resources and support. This work was supported in part by the Offices of NP and HEP within the U.S. DOE Office of Science, the U.S. NSF, the Sloan Foundation, the DFG cluster of excellence ‘Origin and Structure of the Universe’ of Germany, CNRS/IN2P3, FAPESP CNPq of Brazil, Ministry of Ed. and Sci. of the Russian Federation, NNSFC, CAS, MoST, and MoE of China, GA and MSMT of the Czech Republic, FOM and NWO of the Netherlands, DAE, DST, and CSIR of India, Polish Ministry of Sci. and Higher Ed., Korea National Research Foundation, Ministry of Sci., Ed. and Sports of the Rep. of Croatia, and RosAtom of Russia.

References

- [1] T. Matsui, H. Satz, J/ψ suppression by Quark-Gluon Plasma formation, Phys. Lett. B178 (1986) 416. doi:10.1016/0370-2693(86)91404-8.
- [2] S. Digal, P. Petreczky, H. Satz, Quarkonium feed down and sequential suppression, Phys. Rev. D64 (2001) 094015. doi:10.1103/PhysRevD.64.094015.
- [3] A. Mocsy, P. Petreczky, Color screening melts quarkonium, Phys. Rev. Lett. 99 (2007) 211602. doi:10.1103/PhysRevLett.99.211602.
- [4] N. Brambilla, et al., Heavy quarkonium: progress, puzzles, and opportunities, Eur. Phys. J. C71 (2011) 1534. doi:10.1140/epjc/s10052-010-1534-9.
- [5] M. C. Abreu, et al., Transverse momentum distributions of J/ψ , ψ' , Drell-Yan and continuum dimuons produced in Pb+Pb interactions at the SPS, Phys. Lett. B499 (2001) 85–96. doi:10.1016/S0370-2693(01)00019-3.
- [6] A. Adare, et al., J/ψ production vs centrality, transverse momentum, and rapidity in Au+Au collisions at $\sqrt{s_{NN}} = 200$ GeV, Phys. Rev. Lett. 98 (2007) 232301. doi:10.1103/PhysRevLett.98.232301.

- [7] G. Aad, et al., Measurement of the centrality dependence of J/ψ yields and observation of Z production in lead-lead collisions with the ATLAS detector at the LHC, Phys. Lett. B697 (2011) 294–312.
- [8] S. Chatrchyan, et al., Suppression of non-prompt J/ψ , prompt J/ψ , and $\Upsilon(1S)$ in Pb+Pb collisions at $\sqrt{s_{NN}} = 2.76$ TeV, JHEP 1205 (2012) 063. doi:10.1007/JHEP05(2012)063.
- [9] B. Abelev, et al., J/ψ Suppression at forward rapidity in Pb+Pb collisions at $\sqrt{s_{NN}} = 2.76$ TeV, Phys. Rev. Lett. 109 (2012) 072301.
- [10] F. Karsch, R. Petronzio, Momentum distribution of J/ψ in the presence of a Quark-Gluon Plasma, Phys. Lett. B193 (1987) 105. doi:10.1016/0370-2693(87)90465-5.
- [11] Y.-p. Liu, Z. Qu, N. Xu, P.-f. Zhuang, J/ψ Transverse momentum distribution in high energy nuclear collisions at RHIC, Phys. Lett. B678 (2009) 72–76.
- [12] X. Zhao, R. Rapp, Charmonium in medium: From correlators to experiment, Phys. Rev. C82 (2010) 064905.
- [13] H. Liu, K. Rajagopal, U. A. Wiedemann, An AdS/CFT calculation of screening in a hot wind, Phys. Rev. Lett. 98 (2007) 182301. arXiv:hep-ph/0607062, doi:10.1103/PhysRevLett.98.182301.
- [14] R. Sharma, I. Vitev, High transverse momentum quarkonium production and dissociation in heavy ion collisions, arXiv:1203.0329.
- [15] B. I. Abelev, et al., J/ψ production at high transverse momentum in $p + p$ and Cu+Cu collisions at $\sqrt{s_{NN}} = 200$ GeV, Phys. Rev. C80 (2009) 041902.
- [16] K. Ackermann, et al., STAR detector overview, Nucl. Instrum. Meth. A499 (2003) 624–632. doi:10.1016/S0168-9002(02)01960-5.
- [17] W. Llope, et al., The TOFp/pVPD time-of-flight system for STAR, Nucl. Instrum. Meth. A522 (2004) 252–273. doi:10.1016/j.nima.2003.11.414.

- [18] M. Beddo, et al., The STAR barrel electromagnetic calorimeter, Nucl. Instrum. Meth. A499 (2003) 725–739. doi:10.1016/S0168-9002(02)01970-8.
- [19] B. I. Abelev, et al., Systematic measurements of identified particle spectra in $p + p$, d +Au and Au+Au Collisions from STAR, Phys. Rev. C79 (2009) 034909. doi:10.1103/PhysRevC.79.034909.
- [20] A. Adare, et al., Transverse momentum dependence of J/ψ polarization at midrapidity in $p + p$ collisions at $\sqrt{s} = 200$ GeV, Phys. Rev. D82 (2010) 012001. doi:10.1103/PhysRevD.82.012001.
- [21] M. Anderson, et al., The STAR time projection chamber: A unique tool for studying high multiplicity events at RHIC, Nucl. Instrum. Meth. A499 (2003) 659–678. doi:10.1016/S0168-9002(02)01964-2.
- [22] Z. Tang, J/ψ production at high transverse momentum in $p+p$ and A+A collisions, Ph.D. thesis, University of Science and Technology of China, http://drupal.star.bnl.gov/STAR/files/Tang_Zebo.pdf (2009).
- [23] B. Bonner, et al., A single Time-of-Flight tray based on multigap resistive plate chambers for the STAR experiment at RHIC, Nucl. Instrum. Meth. A508 (2003) 181–184. doi:10.1016/S0168-9002(03)01347-0.
- [24] J. Adams, et al., Open charm yields in d +Au collisions at $\sqrt{s_{NN}} = 200$ GeV, Phys. Rev. Lett. 94 (2005) 062301. doi:10.1103/PhysRevLett.94.062301.
- [25] J. Adams, et al., $K(892)^*$ resonance production in Au+Au and $p + p$ collisions at $\sqrt{s_{NN}} = 200$ GeV at STAR, Phys. Rev. C71 (2005) 064902. doi:10.1103/PhysRevC.71.064902.
- [26] J. Adams, et al., Transverse momentum and collision energy dependence of high p_T hadron suppression in Au + Au collisions at ultrarelativistic energies, Phys. Rev. Lett. 91 (2003) 172302. doi:10.1103/PhysRevLett.91.172302.
- [27] K. Nakamura, et al., Review of particle physics, J. Phys. G G37 (2010) 075021, branching ratio for $J/\psi \rightarrow e^+e^-$ is $(5.94 \pm 0.06)\%$, including $(0.88 \pm 0.14)\%$ for $J/\psi \rightarrow \gamma e^+e^-$. doi:10.1088/0954-3899/37/7A/075021.

- [28] Y.-Q. Ma, K. Wang, K.-T. Chao, A complete NLO calculation of the J/ψ and ψ' production at hadron colliders, Phys. Rev. D84 (2011) 114001, and private communication (2012). The color-octet model describes the J/ψ production process as having the quantum number of the color configuration at the intermediate state different from that of the J/ψ . doi:10.1103/PhysRevD.84.114001.
- [29] A. D. Frawley, T. Ullrich, R. Vogt, Heavy flavor in heavy-ion collisions at RHIC and RHIC II, Phys. Rept. 462 (2008) 125–175, and R. Vogt private communication (2009). The color evaporation model is motivated by the principle of quark-hadron duality. It assumes that every produced $c\bar{c}$ evolves into charmonium if it has an invariant mass less than the threshold for producing a pair of open charm mesons. The nonperturbative probability for the $c\bar{c}$ to evolve into a charmonium state is given by an energy-momentum and process independent constant. doi:10.1016/j.physrep.2008.04.002.
- [30] P. Artoisenet, et al., Upsilon production at the Tevatron and the LHC, Phys. Rev. Lett. 101 (2008) 152001, and J. P. Lansberg private communication (2009). The color-singlet model describes the J/ψ production process as having the quantum number of the color configuration at the intermediate state the same as that of J/ψ . doi:10.1103/PhysRevLett.101.152001.
- [31] T. Sjostrand, S. Mrenna, P. Skands, PYTHIA 6.4 physics and manual, JHEP 0605 (2006) 026.
- [32] T. Sjostrand, S. Mrenna, P. Z. Skands, A brief introduction to PYTHIA 8.1, Comput. Phys. Commun. 178 (2008) 852–867. doi:10.1016/j.cpc.2008.01.036.
- [33] M. Bedjidian, et al., hep-ph/0311048 and R. Vogt private communication (2004).
- [34] M. Cacciari, P. Nason, R. Vogt, QCD predictions for charm and bottom production at RHIC, Phys. Rev. Lett. 95 (2005) 122001. doi:10.1103/PhysRevLett.95.122001.
- [35] S. Margetis, Heavy Flavor Tracker (HFT): The new silicon vertex detector for the STAR experiment at RHIC, Nucl. Phys. B (Proc. Suppl.) 210-211 (2011) 227–230.

- [36] D. Acosta, et al., Measurement of the J/ψ meson and b -hadron production cross sections in $p + \bar{p}$ collisions at $\sqrt{s} = 1960$ GeV, Phys. Rev. D71 (2005) 032001. doi:10.1103/PhysRevD.71.032001.
- [37] G. Aad, et al., Measurement of the differential cross-sections of inclusive, prompt and non-prompt J/ψ production in proton-proton collisions at $\sqrt{s} = 7$ TeV, Nucl. Phys. B850 (2011) 387–444. doi:10.1016/j.nuclphysb.2011.05.015.
- [38] V. Khachatryan, et al., Prompt and non-prompt J/ψ production in $p + p$ collisions at $\sqrt{s} = 7$ TeV, Eur. Phys. J. C71 (2011) 1575. doi:10.1140/epjc/s10052-011-1575-8.
- [39] Z. Tang, et al., Spectra and radial flow at RHIC with Tsallis statistics in a Blast-Wave description, Phys. Rev. C79 (2009) 051901.
- [40] Z. Tang, L. Yi, L. Ruan, M. Shao, H. Chen, et al., Statistical origin of Constituent-Quark scaling in the QGP hadronization, Chin. Phys. Lett. 30 (2011) 031101.
- [41] G. Agakishiev, et al., Identified hadron compositions in $p+p$ and Au+Au collisions at high transverse momenta at $\sqrt{s_{NN}} = 200$ GeV, Phys. Rev. Lett. 108 (2012) 072302. doi:10.1103/PhysRevLett.108.072302.
- [42] B. I. Abelev, et al., Identified baryon and meson distributions at large transverse momenta from Au+Au collisions 200 GeV, Phys. Rev. Lett. 97 (2006) 152301. doi:10.1103/PhysRevLett.97.152301.
- [43] A. G. Clark, et al., Inclusive π^0 production from high-energy $p + p$ collisions at very large transverse momenta, Phys. Lett. B74 (1978) 267. doi:10.1016/0370-2693(78)90570-1.
- [44] J. Adams, et al., Identified hadron spectra at large transverse momentum in $p + p$ and $d + Au$ collisions at $\sqrt{s_{NN}} = 200$ GeV, Phys. Lett. B637 (2006) 161–169. doi:10.1016/j.physletb.2006.04.032.
- [45] J. Adams, et al., Pion, kaon, proton and anti-proton transverse momentum distributions from $p + p$ and $d+Au$ collisions at $\sqrt{s_{NN}} = 200$ GeV, Phys. Lett. B616 (2005) 8–16.

- [46] A. Adare, et al., Inclusive cross section and double helicity asymmetry for π^0 production in $p + p$ collisions at $\sqrt{s} = 62.4$ GeV, Phys.Rev. D79 (2009) 012003. doi:10.1103/PhysRevD.79.012003.
- [47] Y. Liu, N. Xu, P. Zhuang, J/ψ elliptic flow in relativistic heavy ion collisions, Nucl. Phys. A834 (2010) 317c–319c. doi:10.1016/j.nuclphysa.2010.01.008.
- [48] L. Adamczyk, et al., Measurement of J/ψ azimuthal anisotropy in Au+Au collisions at $\sqrt{s_{NN}} = 200$ GeV, arXiv:1212.3304.
- [49] S. Chatrchyan, et al., Indications of suppression of excited Υ states in Pb+Pb collisions at $\sqrt{s_{NN}} = 2.76$ TeV, Phys. Rev. Lett. 107 (2011) 052302. doi:10.1103/PhysRevLett.107.052302.
- [50] S. Chatrchyan, et al., Observation of sequential Upsilon suppression in Pb+Pb collisions, Phys.Rev.Lett. 109 (2012) 222301. doi:10.1103/PhysRevLett.109.222301.
- [51] J. Wiechula, Nuclear modification of J/ψ production in Pb+Pb collisions at $\sqrt{s_{NN}} = 2.76$ TeV, arXiv:1208.6566.
- [52] H. Yang, Elliptic flow of J/ψ at forward rapidity in Pb+Pb collisions at 2.76 TeV with the ALICE experiment, arXiv:1211.0799.